Wideband Phased Array Antenna Design with Fragmented Combiner Technology

David W. Landgren, Theresa Brunasso, James B. Dee, Jonathan Perez,
Daniel J.P. Dykes, Jeramy M. Marsh, Charles P. Hunter, and Kenneth W. Allen*

***Abstract*—In this work, a novel fragmented combiner network is designed to excite a planar phased array antenna, comprised of 4x4 elements with a single RF port (i.e. 16:1). The antenna system, intended for receive (Rx) applications, was engineered with ultra-wideband (UWB) performance that covers portions of the L-, S-, and C-bands. The unit cell design consists of a printed circuit board (PCB) stack-up with a driven aperture layer that is DC connected with a single metal pin to a fragmented combiner layer. This single connection indicates that the antenna is unbalanced and therefore no balun or differential amplifier is required. Additionally, there are no vias required for this unbalanced array, allowing for this concept to be easily scaled to lower or higher frequencies. Further, the fragmented combiner is a PCB-based component, which eliminates the need for traditional commercial-off-the-shelf (COTS) components e.g. Wilkinson chips for this specific application. The simulated results of this unbalanced phased array with a fragmented combiner network are discussed and experimentally validated.**

I. Introduction

In recent years, the U.S. government has auctioned-off portions of the electromagnetic spectrum, e.g. AWS-3 sell-off of 65 MHz of the L-band spectrum for a collective price tag of 45B USD. Consequently, a transition of certain government systems is occurring from L-band to higher frequencies such as S- and C-band. This desire to operate at higher frequencies with greater fractional bandwidth provides the impetus for hardware developments with the antenna systems. This work is concentrated on the telemetry application of fire-control radar testing, which requires an instantaneous bandwidth capable of covering the legacy frequency band (L-band) up to previously unused frequencies (C-band) with sufficient gain to close the link down range, i.e. 10-20 dBi.

In parallel to the spectrum sell-off, there have been technological developments with planar unbalanced arrays [1–11]. Unbalanced arrays have the advantage, over traditional designs with differentially-fed elements, that the number of RF-connections are reduced by a factor of two due to the single feed point for the embedded elements. However, differentially fed elements have the benefit of equal amplitude excitation with 180-degree phase difference for efficient current distributions, in terms of radiation, on the aperture which is capable of achieving the area gain limit over UWBs [12]. In an attempt to regain this loss in efficiency, complex architectures were developed with vias strategically placed through the antenna stack-up. These so-called planar unbalanced modular arrays (PUMA) have demonstrated efficient radiation for dual-polarization operation up to 6:1 bandwidths [8].

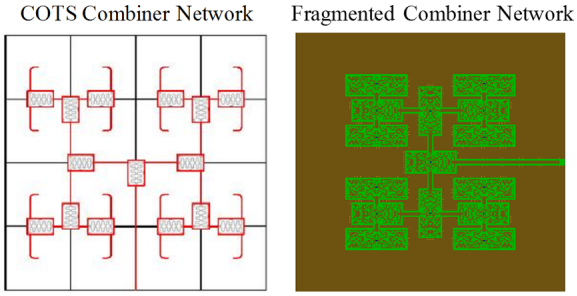

Figure 1. Comparison of (left) a traditional combiner network with commercial-off-the-shelf (COTS) Wilkinson chips and (right) a fragmented combiner network. Both are designed for a 4x4 array with the same footprint for a 16:1 network.

In this work, we reduce the complexity of the apertures unit cell by removing the vias and adding a parasitic layer into the stack-up. Therefore, aside from the feed structure, this is a planar stack-up. The novel aspect of this work is the fragmented combiner network. The unbalanced feeding scheme reduces the number of RF connections to 16 for the 4x4 array. We leverage a genetic algorithm that is coupled with finite-difference time-domain (FDTD) simulations to optimize the fragmented combiner, shown in Fig. 1, such that the insertion losses are minimized and equal amplitude excitation is provided for the elements of the antenna array. Experimental studies are performed to validate the simulations of the fragmented combiner and overall antenna architecture.

K.W. Allen et al. are with the Georgia Institute of Technology, Georgia Tech Research Institute, Advanced Concepts Laboratory, Atlanta, GA, 30318 USA. *Corresponding author email: Kenneth.Allen@gtri.gatech.edu, T. Brunasso is with D&S Microwave Inc., Snellville, GA, 30078 USA.

978-1-5386-6557-2/18/$31.00 ©2018 IEEE

II. Fragmented Optimization

A. Optimization Process

In this work, we aim to design an efficient combiner network that leverages a fragmented metallic pattern on a dielectric substrate. Computational electromagnetic (CEM) codes, such as FDTD solvers, coupled with genetic algorithms have been demonstrated to be effective at the characterization and design of electromagnetic structures [13–19]. The genetic algorithm, mimicking evolutionary processes, evaluates the populations and selects the best fit designs to propagate to the next population of design candidates with some mutations. The general process involves various parameters that can be altered, such as toggling between metallic and dielectric subwavelength areas, which are encoded as bits. The string of bits translates to a specific configuration of the fragmented pattern of the combiner network. The individual designs are scored against the mathematical description of the desired performance for a metric (e.g., insertion loss, amplitude at a specific port, etc.) over the frequency range of interest (i.e., 1.4-6.7 GHz). The form factor is determined by the specifications of the telemetry antenna. This design process is shown in Fig. 2.

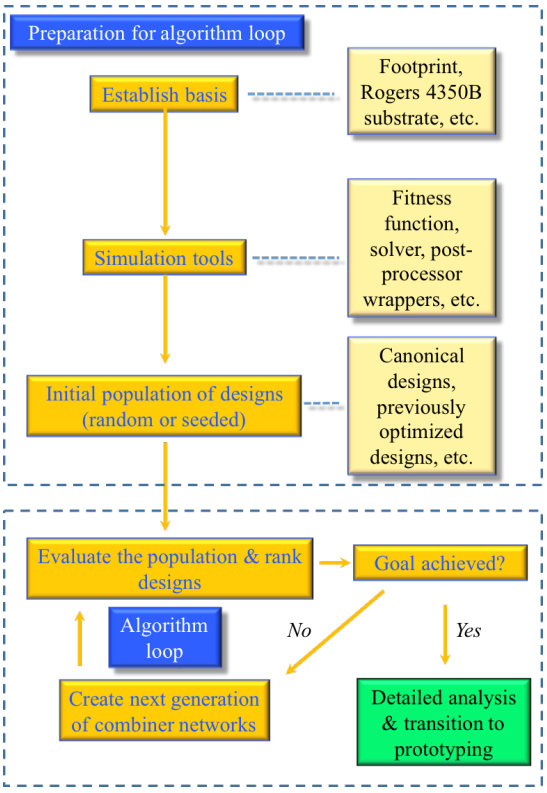

Figure 2. Illustration of the design process, representing the case of the fragmented combiner.

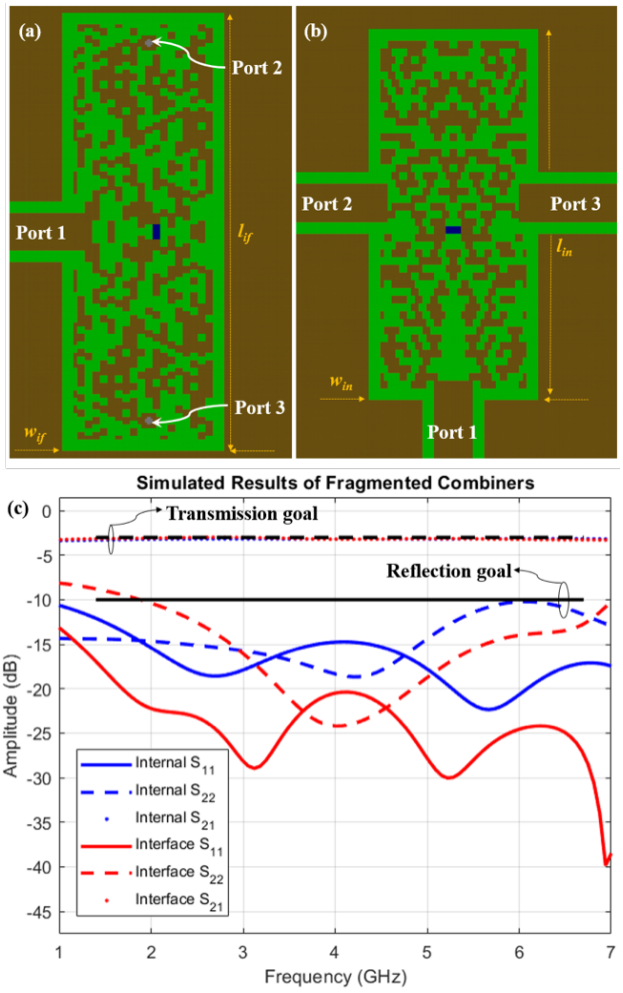

Figure 3. Computational models of the two fragmented combiner types: (a) interfacial and (b) internal, where bronze, green, and blue represents metal, dielectric, and resistive sheets, respectively. (c) Simulated results of the optimized fragmented combiners.

In this case, to achieve maximum power efficiency in the given space, it was necessary to design two separate combiners: i) interfaces the unbalanced antenna feed structure [Fig. 3(a)] with a microstrip transmission line and ii) to provide an internal combiner [Fig. 3(b)]. A collection of these two logical units are arranged to form the 16:1 combiner for the 4x4 array, as shown in Fig. 1(b). The designs used electrical properties mimicking a 50 mil thick Rogers 4350B board, e.g. ϵ=3.55, with a chip resistor of 50 Ω.The footprint for the two fragmented combiner types is l_{if} x w_{if} = 1100x370 $mils^2$ and l_{in} x w_{in} = 900x380 $mils^2$ for the interfacial and internal combiners, respectively. These regions are pixelated, with pixel sizes of 20x20 $mils^2$, so that the optimizer can tune the fragmented pattern with electrically fine spatial features, i.e. $\lambda_c/147.5$. This level of

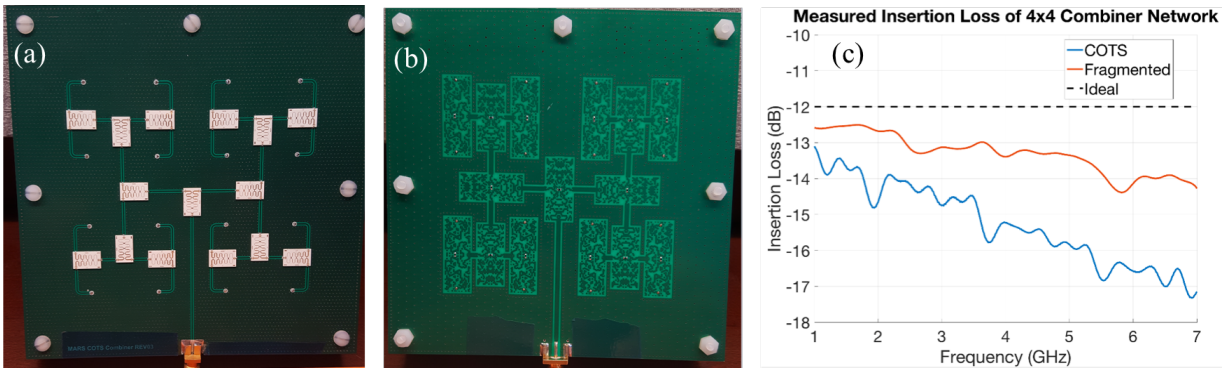

Figure 4. Experimental results of improved performance of a fragmented combiner over a COTS combiner in a 4x4 phased array. (a) COTS combiner with Wilkinson chips and (b) fragmented combiner network. (c) Measured results for a direct comparison of performance.

discretization results in 532 bits and 288 bits for the interfacial and internal combiners, respectively. Although these search spaces are relatively large, an optimized solution was obtained for both cases.

The fitness function consisted of three performance metrics: i) reflections into the combiner, ii) transmission through the combiner to the 50 Ω load, and iii) isolation. Phase was not considered in the fitness function but could be implemented. Reflections at ports 1 and 2 for both combiners (S_{11}) had a goal of -10 dB of reflected amplitude. For the interfacial combiner S_{21}, the goal was -3 dB of transmitted amplitude. The fragmented mask had symmetry, which eliminated the need to also score S_{31}. Also, isolation of the combiners had a goal of 10 dB in amplitude. The optimized designs performance, in terms of scattering parameters, is shown with respect to the goals of the fitness function in Fig. 3(c). The optimizer was able to tune the designs such that the fitness functions were nearly satisfied in all cases. Therefore, these fragmented combiners were chosen for fabrication and experimental characterization. Those results are discussed in the next section.

III. Experimental Results

A. Combiner Measurements

In order to experimentally characterize the COTS combiner design, Fig. 4(a), and fragmented combiner design, Fig. 4(b), the RF connections were terminated with 50-Ω loads. A spectrum analyzer was then used to measure the insertion losses, Fig. 4(c),at the RF port used to excite the RF connections. These measurements demonstrate an advantage for the fragmented combiner technology due to lower insertion losses across the entire band, *L*-band to *C*-band. The ideal insertion loss, no losses, for a 4 to 1 divider is -12 dB with -3 dB at each split in the combiner network. The in-house fragmented aperture combiner network is within 2.5 dB of this ideal goal across the band. These measurements experimentally validate the FDTD simulations of the optimized designs for both combiner networks. It should be noted that phase was not considered for this study.

B. Antenna Measurements

The COTS combiner design, Fig. 4(a), and fragmented combiner design, Fig. 4(b), were integrated with the 4x4 antenna aperture, Fig. 5. Details of the aperture design can be found in ref. [10]. This allows for a direct comparison on the impacts of the two competing combiner technologies on the antenna performance. The two antenna method was used to calibrate and determine the realized gain values of the two designs at broadside, as shown in Fig. 5.

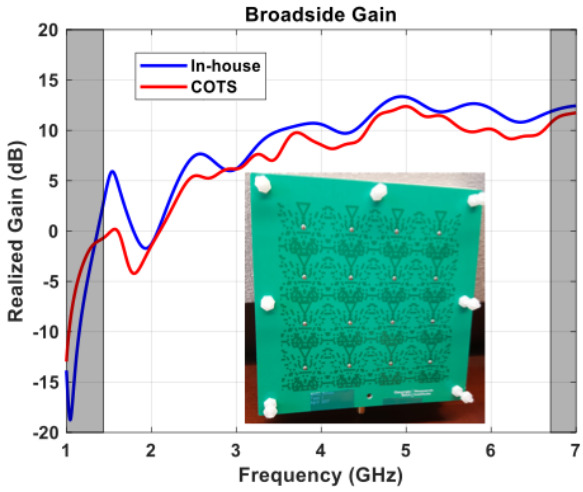

Figure 5. Direct comparison of the in-house fragmented combiner and the COTS combiner in terms of realized gain and broadside. (inset) Driven layer of the 4x4 antenna array.

It is observed, in Fig. 5(b), that the 4x4 antenna array performs with higher realized gain across the entirety of the frequency band of interest (L-band to C-band) for the in-house fragmented combiner in direct comparison with the COTS combiner solution. The physical explanation of this is likely due to the reduced insertion losses of the fragmented combiner, as shown in Fig. 4(c). However, the phase across the elements is also a factor in the directivity of spatial beam profile generated by the phased array.

IV. Conclusions

In this work, we demonstrated a novel fragmented combiner network that outperforms the insertion losses obtained by the COTS solution over the L-, S-, and C-bands. These results provide a simple antenna architecture where the overall antenna stack-up only consists of planar layers; therefore, the design does not require a balun or vias. Further, the fragmented combiner is a PCB-based component, which provides savings in cost. The complete antenna system, unbalanced phased array with a fragmented combiner network, was experimentally validated over the L- , S-, C-bands with ultra-wideband performance (i.e. 4.8:1). Based on these results, a scaled version of this antenna system to a 16x16 array will be sufficient to close the link for the fire-control radar telemetry application.

Acknowledgement

The authors would like to thank Dr. Ryan S. Westafer for stimulating discussions and Mrs. Kathy M. Bowland for internal peer-review of this article. This work was funded in part by the Test Resource Management Center (TRMC) and funded through the Spectrum Access R&D program via Picatinny Arsenal under Contract No. WL5QKN-15-9- 1004. The Executing Agent and Program Manager work out of the Air Force Test Center (AFTC). Any opinions, findings, and conclusions or recommendations expressed in this material are those of the authors and do not necessarily reflect the views of TRMC, the SAR&D Program and/or the Picatinny Arsenal. DISTRIBUTION STATEMENT A. Approved for public release; Distribution is unlimited 412TW-PA-18517.

References

[1] S. S. Holland and M. N. Vouvakis, "Design and fabrication of low-cost puma arrays," in *Antennas and Propagation (APSURSI), 2011 IEEE International Symposium on*. IEEE, 2011, pp. 1976–1979.

[2] S. S. Holland, D. H. Schaubert, and M. N. Vouvakis, "A 7–21 ghz dual-polarized planar ultrawideband modular antenna (puma) array," *IEEE Transactions on Antennas and Propagation*, vol. 60, no. 10, pp. 4589–4600, 2012.

[3] S. S. Holland and M. N. Vouvakis, "The planar ultrawideband modular antenna (puma) array," *IEEE Transactions on Antennas and Propagation*, vol. 60, no. 1, pp. 130–140, 2012.

[4] J. T. Logan and M. N. Vouvakis, "Planar ultrawideband modular antenna (puma) arrays scalable to mm-waves," in *Antennas and Propagation Society International Symposium (APSURSI), 2013 IEEE*. IEEE, 2013, pp. 624–625.

[5] J. T. Logan, S. S. Holland, D. H. Schaubert, R. W. Kindt, and M. N. Vouvakis, "A review of planar ultrawideband modular antenna (puma) arrays," in *Electromagnetic Theory (EMTS), Proceedings of 2013 URSI International Symposium on*. IEEE, 2013, pp. 868–871.

[6] M. Y. Lee, J. T. Logan, R. W. Kindt, and M. N. Vouvakis, "Simplified design of 6? 1 puma arrays," in *Antennas and Propagation & USNC/URSI National Radio Science Meeting, 2015 IEEE International Symposium on*. IEEE, 2015, pp. 2515–2516.

[7] J. Logan, "A new class of improved bandwidth planar ultrawideband modular antenna (puma) arrays scalable to mm-waves," 2013.

[8] J. T. Logan, R. W. Kindt, M. Y. Lee, and M. N. Vouvakis, "A new class of planar ultrawideband modular antenna arrays with improved bandwidth," *IEEE Transactions on Antennas and Propagation*, vol. 66, no. 2, pp. 692–701, 2018.

[9] D. W. Landgren, K. R. Cook, D. J. Dykes, J. Perez, P. R. Bowden, and K. W. Allen, "A wideband mmwave antenna element with an unbalanced feed," in *Aerospace and Electronics Conference (NAECON), 2017 IEEE National*. IEEE, 2017, pp. 209–212.

[10] D. W. Landgren, , D. J. Dykes, and K. W. Allen, "An unbalanced feed design for wideband phased arrays," in *Aerospace and Electronics Conference (NAECON), 2017 IEEE National*. IEEE, 2017.

[11] D. J. Dykes, K. M. Bowland, and K. W. Allen, "Wideband millimeter-wave fragmented aperture antenna," in *Aerospace and Electronics Conference (NAECON), 2017 IEEE National*. IEEE, 2017, pp. 213–216.

[12] H. Wheeler, "Simple relations derived fom a phased-array antenna made of an infinite current sheet," *IEEE Transactions on Antennas and Propagation*, vol. 13, no. 4, pp. 506–514, 1965.

[13] D. S. Weile and E. Michielssen, "Genetic algorithm optimization applied to electromagnetics: A review," *IEEE Transactions on Antennas and Propagation*, vol. 45, no. 3, pp. 343–353, 1997.

[14] Y. Rahmat-Samii and E. Michielssen, "Electromagnetic optimization by genetic algorithms," *Microwave Journal*, vol. 42, no. 11, pp. 232–232, 1999.

[15] M. M. Scott, D. L. Faircloth, J. A. Bean, and K. W. Allen, "Permittivity and permeability determination for high index specimens using partially filled shorted rectangular waveguides," *Microwave and Optical Technology Letters*, vol. 58, no. 6, pp. 1298–1301, 2016.

[16] K. W. Allen, M. M. Scott, D. R. Reid, J. A. Bean, J. D. Ellis, A. P. Morris, and J. M. Marsh, "An x-band waveguide measurement technique for the accurate characterization of materials with low dielectric loss permittivity,"

Review of Scientific Instruments, vol. 87, no. 5, p. 054703, 2016.

[17] K. W. Allen, D. J. Dykes, D. R. Reid, J. A. Bean, D. W. Landgren, R. T. Lee, and D. R. Denison, "Metasurface engineering via evolutionary processes," in *Aerospace and Electronics Conference (NAECON), 2017 IEEE National*. IEEE, 2017, pp. 172–178.

[18] K. W. Allen, D. J. Dykes, K. M. Bowland, and D. W. Landgren, "Metasurface antenna with thermally controlled reconfigurable states: a simulation study," in *Aerospace and Electronics Conference (NAECON), 2017 IEEE National*. IEEE, 2017, pp. 1–4.

[19] J. M. Kovitz and K. W. Allen, "Recent developments toward reconfigurable mmwave apertures and components using vanadium dioxide rf switches," in *Wireless and Microwave Technology Conference (WAMICON), 2018 IEEE 19th*. IEEE, 2018, pp. 1–4.